

# Comparison of Mathematical Surface Energy Models and Fuzzy Approach Pertaining to Surface Energy Level of Polylactic Acid and Linear Low-density Polyethylene

Shanmugapriya ELANGOVA<sup>1\*</sup>, Thendral Thiyaku THIYAGU<sup>2</sup>,  
Hariharan PERIANNAPILLAI<sup>3</sup>, Baskar SUBRAMANIAN<sup>4</sup>

<sup>1</sup> Department of Computer Science and Engineering, College of Engineering Guindy, Anna University Chennai, 600025, Tamil Nadu, India

<sup>2</sup> Department of Printing and Packaging Technology, College of Engineering Guindy, Anna University Chennai, 600025, Tamil Nadu, India

<sup>3</sup> Department of Manufacturing Engineering, College of Engineering Guindy, Anna University Chennai, 600025, Tamil Nadu, India

<sup>4</sup> Department of Mechanical Engineering, Rajalakshmi Engineering College, Chennai, 602105, Tamil Nadu, India

<http://doi.org/10.5755/j02.ms.38910>

Received 24 September 2024; accepted 11 June 2025

The usage of flexible film in the food packaging industries has been rapidly increasing over the past few years. In flexible printing process, the wettability and adhesion of polymer substrates depend on the surface composition, roughness, energy level and tension. Among all these properties, the Surface Energy Level (SEL) of polar and nonpolar polymer substrates were determined by measuring Contact Angle Values (CAV). This study focuses on experimentation based SEL measurement using corona treatment for both treated and untreated LLDPE (Linear Low-Density Poly Ethylene) and PLA (Polylactic Acid) films using MSEM (Mathematical Surface Energy Models) such as Fowkes, Owens-Wendt, and Wu based on the CAV of polymer films and further to develop a Mamdani fuzzy interface-based model for predicting optimum SEL with help of experimentally generated data. The observed SEL of untreated and treated PLA and LLDPE films were 40 and 38, 48 and 44 mN/m respectively. Fuzzy-based simulations showed similar results, with treated PLA and LLDPE at 45.4 and 44. Finally, the proposed Mamdani model can predict SEL with high accuracy in comparison with experimental results and the good printability of ink adhesion was achieved in treated than the untreated films.

*Keywords:* polymers, biopolymers, surface energy, printing, fuzzy logic.

## 1. INTRODUCTION

Plastics are often used in printing and packaging applications due to their intrinsic characteristics. The polymer materials that are widely used in printing and packaging applications are Polyethylene (PE), Polyethylene terephthalate (PET), Polypropylene (PP), and Polyvinyl chloride (PVC) [1]. However, usage of polymer films in printing applications without surface treatment has several disadvantages, such as poor printability, poor wettability, and poor adhesion [2–4]. These characteristics are strongly connected to low SEL of the polymer films. It is observed that maintaining sufficient surface tension and surface energy is a crucial characteristic of flexible polymer films used in printing applications [5–8]. Consequently, the most popular techniques for improving the SEL of polymer films used in printing and packaging include chemical, UV, flame, plasma, and corona treatments [9, 10]. To ensure outstanding printability, the ink's surface tension and the polymer materials surface energy must be maintained at optimal levels. In general, SEL of polymer substrates is measured by the CAV of flexible polymer film using a variety of Mathematical Surface Energy models (MSEM), including Fowkes, Owens-Wendt, and Wu. Using these MSE models to analyze the SEL of polymer films has

several benefits, but experimentally based SEL assessment has some drawbacks, including uncertainty, imprecision, time consumption, and increased manufacturing costs. To overcome this, the optimum SEL for the polymer film surface is estimated using a data-driven fuzzy modelling approach, which also ensures good printability in flexible films. Many research literatures were reported in predicting the performance of engineering materials by using computational techniques and built best predictive modelling. [11] constructed prognostic models to determine the optimal parameters by selecting factors such as parameters of printing plate, the rheological parameters of ink, the lineature of anilox roller and surface properties of materials to be printed on the quality of flexographic printing process using fuzzy logic tools. [12] employed fuzzy logic technique to predict the hardness of composite materials and compared experimental results for better accuracy. [13] used the sessile drop method to explore the mechanisms of action of various surface energy models, including Wu, Oss-Chaudhury-Good (VOGC), Fowkes, Owens-Wendt-Rabel-Kaelble (OWRK), and Van. Finally, it was found that inadequate wettability during adhesion, cohesive forces in wetting processes, and cohesion forces in the liquid phase dominated adherence to the substrate. [14] developed the Taguchi methodology, to predict the hardness

---

\*Corresponding author: S. Elangovan  
E-mail: [espriyase@annauniv.edu](mailto:espriyase@annauniv.edu)

of engineering materials, to mathematical modelling, proved relatively low average error levels. La, [15] employed Artificial Neural Network (ANN) models to forecast SEL, a crucial parameter in both scientific and industrial applications. To improve predictive modelling in this field, this technique is utilized to estimate optimums SEL, demonstrating the growing confluence of material science and artificial intelligence. [16] constructed fuzzy model for predicting the mechanical characteristics of a composite material made of polymers. The fuzzy model was validated through the construction of membership functions and a series of test case investigations. [17] have investigated the mechanical properties of a recently developed HDPE polymer composite material Neuro-fuzzy modelling was used to compare the experimental results with the theoretical estimate of the properties of the polymer composite to determine the ideal mechanical properties. The experimental investigation and the theoretical research agreed well.

In this context, several well-known Artificial Intelligence (AI) techniques such as Fuzzy Logic (FL), Machine Learning (ML), Artificial Neural Networks (ANN), Adaptive Neuro Fuzzy Inference System (ANFIS), Support Vector Regression and Genetic Programming are being used to develop relationship between given input parameters and output responses [18, 19]. Among these schemes, FL possesses the ability to model a complex process containing uncertain and vague information with less hardware and software resources [20, 21]. FL is a highly flexible and non-linear modelling technique for experimental data involving certain uncertainties between the relationships of input process variables and output responses. Mamdani fuzzy logic method is used in this study due to its flexibility and adaptable framework for estimating or predicting SEL for sustainable and synthetic polymer materials. Utilizing Mamdani based fuzzy logic to combine the rules framed by fuzzy logic and observe the output from fuzzy for the overall solutions of food packaging attributes [22]. In addition to this, most of the researchers were conducted surface free energy experiments in the solid powders [23, 24].

To prevent contamination of the environment, numerous researchers are currently working on developing biopolymer flexible polymer film [25, 26]. Because PLA is more transparent, has a higher tensile strength, and is as rigid as PET film, it is utilized in a variety of flexible packaging applications among other biopolymer materials [27–29]. This study uses three MSE models based on the CAV of the polymer surface to measure the untreated and treated SEL of both films. To improve prediction, the experimental findings are compared with the FL System. The two films were then examined for printability using a flexographic proofer with UV inks, where a variety of tests, including adhesion, dyne, density, and rub resistance tests, were used to assess the print quality. Finally, a comparison of PLA and LLDPE films print quality is made for real-world field applications. [30]. According to previous literatures reported, there was no research has been reported on predicting SEL in flexible film with fuzzy logic based data driven methods. However, there were few researches focused on implementation of computational techniques for the prediction of direct ink writing of 3D printable material

formulations. [31], additively manufactured polymer composites [32], numerical methods for design and testing of additively manufactured materials [33], modelling effect of slurry impacts on 3D printed PLA materials [34], and mechanical properties of 3D printed materials [35]. To fill this research gap, a novel approach is implemented to predict the SEL of polymer films used in printing applications.

## 2. MATERIALS AND METHODS

### 2.1. Materials

The blown films were made with the LLDPE and PLA resins. Thermofisher Scientific's HAAKE Poly Lab QC single screw blown film extruder was used to take two polymer films. The thickness of the films was maintained between the ranges of 80–100 microns and measured by using the Mitu-Toyo film thickness gauge. TOYO INKS Corporation donated INSTACURE UV 111 PROCESS MAGENTA series, a UV curable ink. These inks are solvent-free, chemical resistance, short time curing, and have excellent adhesion strength on most of the film substrate. The surface tension of ink was 25–30 mN/m.

### 2.2. Surface treatment and printing

Surface corona treatment was performed by using ENERCON COMPAK™ 2000 [11]. The PLA and LLDPE films of 20 × 22 cm size are cut down and taken for surface treatment. It uses the electric charge (500–1500 watt/m<sup>2</sup>) to change the chemical properties of the material placed within the energy stream. Treatment was done on a single side with the machine of the following setup of 0.60 kW (power), 8 m/min (line speed). Finally, the treated films were subjected for the flexography printing process for further print quality analysis.

### 2.3. Dyne pen test

Dyne pen test commonly referred to as Corona test liquids, are used to detect surface energy very efficiently and easily. This measurement method is predicated on ISO 8296 [36]. A mixture of Ethyl cellosolve and formamide solution is used to determine the surface energy level of polymer films. The cotton applicator method is used to test the surface energy of the substrate. A few drops of calibrated dyne ink solution are placed in the tip of a clean cotton applicator. The dyne ink solution of 36, 40, 44, 48 and 52 dynes/cm is spread lightly over the treated and untreated samples.

### 2.4. Measurement of CAV

The CAV of the films was measured at 20<sup>o</sup> using Goniometer as per ASTM D5946 standard. The hydrophobic films by contact angles greater than 90 degrees, indicating lower surface energy and hydrophilic films were confirmed by contact angles less than 90 degrees, indicating higher surface energy. This imparts good wettability and adhesion polymer film substrate.

### 2.5. Surface energy models

The SEL and wettability determines printability of the polymer films. SEL can be theoretically determined by

using several MSE models. The proposed work utilized Fowkes model, [37] Owens–Wendt model [38] and Wu model to calculate the surface energy of both treated and untreated PLA and LLDPE from the observed CAV. The suggested models split the total surface energy into two parts: surface energy resulting from polar and dispersive interactions in the film surface.

### 2.5.1. Fowkes model

The Fowkes model [39] divides the surface energy of liquids and solids into their polar and dispersive components by combining the Young and Young-Dupree equations. In a thermodynamical equilibrium, Young equation shows:

$$\gamma_S = \gamma_{SL} + \gamma_L \cos\theta. \quad (1)$$

The interfacial tension between a liquid and a solid polymer can then be evaluated by

$$\gamma_{SL} = \gamma_S + \gamma_L - 2 \left[ (\gamma_L^d \gamma_S^d)^{\frac{1}{2}} + (\gamma_L^p \gamma_S^p)^{\frac{1}{2}} \right], \quad (2)$$

where  $\gamma_S$  is the surface energy of the solid;  $\gamma_{SL}$  is the interfacial tension between the solid and the liquid;  $\gamma_L$  is the surface tension of the liquid;  $\gamma_S^d$  and  $\gamma_S^p$  are the dispersion and polar components of the surface energy of the solid;  $\gamma_L^d$  and  $\gamma_L^p$  are the dispersion and polar components of the surface tension of the liquid.

Using Eq. 1 and Eq. 2 can be in the form of the total surface energy of a solid, can be expressed as the sum of polar and dispersive components as follows:

$$\gamma_S = \gamma_S^d + \gamma_S^p. \quad (3)$$

### 2.5.2. Owens-Wendt (extended Fowkes) model

The Owens-Wendt model [8], which combines Young's equation with Fowkes' theory, could be used to express the OWRK equation as follows:

$$\gamma_L(1 + \cos\theta) = 2\sqrt{\gamma_L^d \gamma_S^d} + 2\sqrt{\gamma_L^p \gamma_S^p}. \quad (4)$$

### 2.5.3. Wu model

Wu [40] developed an equation that takes into account harmonic rather than geometric means for polar and dispersive liquid interaction that takes place on a polymer surface using the idea of OWRK.

$$\gamma_{SL} = \gamma_S + \gamma_L - 4 \left[ \frac{\gamma_S^d \gamma_L^d}{\gamma_S^d + \gamma_L^d} + \frac{\gamma_S^p \gamma_L^p}{\gamma_S^p + \gamma_L^p} \right]. \quad (5)$$

### 2.5.4. Density

A spectrophotometer (X-Rite 528 GmbH, Germany) was used to analyze the print density of the film samples. USING the ASTM E308 standard, the spectral reflectance value of each film sample was calculated and converted into CIELAB colorimetric coordinates ( $L^*$ ,  $a^*$ , and  $b^*$ ). For each film sample, measurements were conducted at three distinct points, and an average value was given as the result.

### 2.5.5. Rub resistance

The rub resistance of the film samples was studied after 2–3 weeks after printing process using Sutherland Ink Rub Tester (Micro digital model, make: Linux) with reference to

ASTM D5264. The trimmed printed film samples were placed on the rubber base pad and the test area of film is subjected to 2 or 4 lbs weight which automatically rubbed over 20 cycles repeatedly on the film surface and the number of cycles was set on the timer. Then the printed film strip sample was removed from the rubber pad and rub resistance against given load was assessed for actual ink degradation/ink faded. The condition is maintained at  $23 \pm 2^\circ\text{C}$  and  $50 \pm 5\%$  RH for not less than 24 h prior to test.

### 2.5.6. Tape peel off adhesion test

Using 3M #610 or Sellotape office adhesive tape test, the adhesion of dried ink to the film sample was studied which strongly adhered to the print and are quickly pulled off manually followed by ASTM F2252-03 standard. For each film sample, a test was performed on two different strips, after the printing process. The adhesion was measured by analyzing images of the tape strips ( $6.2\text{ cm} \times 1.8\text{ cm}$ ) applied to the printed film sample and the physical observation was carried out for ink transfer onto the tape. The condition is maintained at  $23 \pm 2^\circ\text{C}$  and  $50 \pm 5\%$  RH for not less than 24 h prior to the test. This test can be used to assess ink-to-substrate adhesion when ink flaking happens with uncured or readily ablated inks.

## 3. DEVELOPMENT OF THE MODEL

In fuzzy system, fuzzy rules are utilized to find the output parameter SEL by using the input parameters such as polarity ( $p$ ) and dispersivity ( $d$ ) of  $SE$ . The selection of membership function ( $mf$ ) is not depending on the any specific method. In this study, triangular membership function is utilized to find the operating parameters [41]. The rules are developed in the form of linguistic terms. The output response is predicted by using Mamdani fuzzy inference system. In general, the one rule will be developed based on expert system and knowledge of human beings and for one experimentation. The eight fuzzy rules are developed according to the characteristics of SE of flexible film [42].

The thirteen fuzzy rules in the form of linguistic terms for treated and untreated polymer film developed based on Response Surface Methodology (RSM) based Box-Behnken design (BBD) is a statistical tool used to analyze and optimize complex systems with multiple variables:

- Rule 1 if Put is mf1 and dut is mf1 then SEut is mf1
- Rule 2 if Put is mf3 and dut is mf2 then SEut is mf5
- Rule 3 if Put is mf2 and dut is mf2 then SEut is mf4
- Rule 4 if Put is mf3 and dut is mf1 then SEut is mf3
- Rule 5 if Put is mf2 and dut is mf2 then SEut is mf4
- Rule 6 if Put is mf2 and dut is mf1 then SEut is mf2
- Rule 7 if Put is mf2 and dut is mf2 then SEut is mf4
- Rule 8 if Put is mf1 and dut is mf3 then SEut is mf6
- Rule 9 if Put is mf3 and dut is mf3 then SEut is mf8
- Rule 10 if Put is mf2 and dut is mf3 then SEut is mf7
- Rule 11 if Put is mf2 and dut is mf2 then SEut is mf4
- Rule 12 if Put is mf2 and dut is mf2 then SEut is mf4
- Rule 13 if Put is mf2 and dut is mf2 then SEut is mf4

Out of 13 rules, 8 rules were different and remaining 5 rules were same. For treated film, same 13 rules developed as similar with the untreated film. These rules were developed with respect to the experimental values of the SEL of flexible film. For defuzzification process, a centroid method is employed to predict the values of SEL as illustrated in Eq. 9. This procedure has been carried out with fuzzy logic designer tool box presented in MATLAB.

$$SE_f = \frac{\sum_i^n A(\theta_i) f_i}{\sum_i^n A(\theta_i)}, \quad (6)$$

where  $SE_f$  is the fuzzy controller output of the surface energy of bio thin film,  $A(\theta_i)$  is the centroid of specific rule utilized in the fuzzy rule and  $n$  is the summation of rules developed for specific application.

## 4. RESULTS AND DISCUSSION

### 4.1. Printability of treated and untreated flexible film

#### 4.1.1. Dyne pen testing and surface morphology

SEL of flexible PLA and LLDPE film is evaluated by using various dyne pens (36, 38, 40, 42, 44, 46, 48, 50 and 52 dynes/cm) dragged over the polymer surface of both the materials [43]. The good surface adhesion was found at the dyne pen 40 for untreated PLA and 36 for untreated LLDPE. Then, both polymer substrates were subjected to the corona treatment for surface modification and observed dyne values for both treated PLA and LLDPE are 48 and 44 dynes/cm respectively as shown in Fig. 1. Finally, it was inferred that the enhanced SEL of treated PLA and LLDPE film is expected to have good wettability of ink over the polymer surface. According to the experiment and fuzzy logic simulation, the treated and untreated PLA and LLDPE film dyne values are shown in Table 1.

**Table 1.** Dyne values

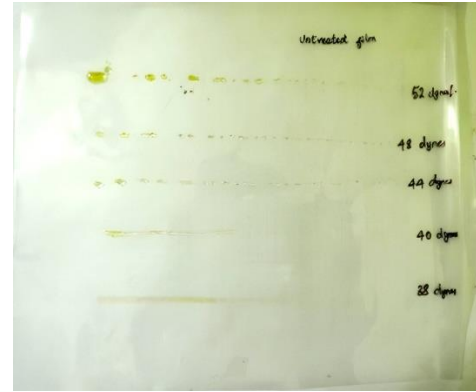
Films	Untreated, mN/m		Treated, mN/m	
	Experiment	Fuzzy logic	Experiment	Fuzzy logic
PLA	40	40	48	45.4
LLDPE	36	38	44	44

Fig. 2 displays SEM (S-4800, Hitachi, Japan) images of untreated/treated PLA and LLDPE film samples both before and after corona treatment. The printed results observed from untreated PLA and LLDPE films were obviously undesirable due to the low ink wettability in the film surface [28]. As a result, the films were subjected to electrical discharge at 500, 1000, and 1,500 watt-min/m<sup>2</sup>. It was found that the corona discharge at 1,000 watt-min/m<sup>2</sup> revealed 48 and 44 mN/m respectively.

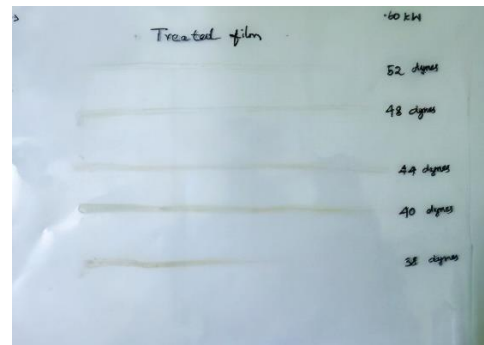
#### 4.1.2. Evaluating SEL using surface energy models

Based on the observed results, it was concluded that water has a higher CAV than ethylene glycol because it has a higher surface tension. Using various calculation models, the estimated CAV values of the polar and dispersive components of PLA and LLDPE films that had been treated and those that had not were determined. The surface energy of the polar and dispersive components of the treated and

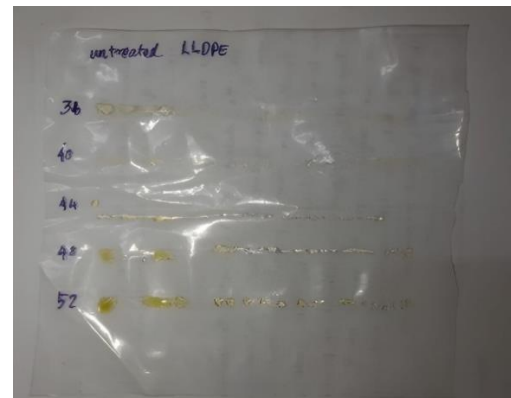
untreated PLA and LLDPE films were calculated by using CAV as shown in Fig. 3 and Fig. 4.



a



b



c



d

**Fig. 1.** Surface adhesion of various dyne pen of: a – untreated PLA; b – treated PLA; c – untreated LLDPE; d – treated LLDPE films

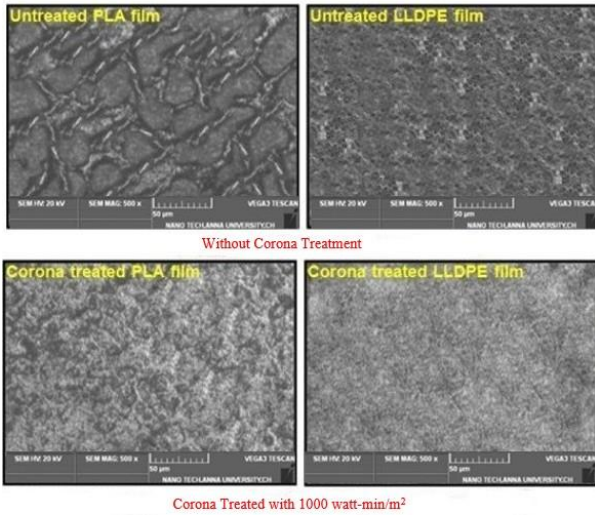


**Fig. 2.** Morphology of PLA and LLDPE film surface comparison (before and after corona surface treatment) with a scale bar of 50 microns

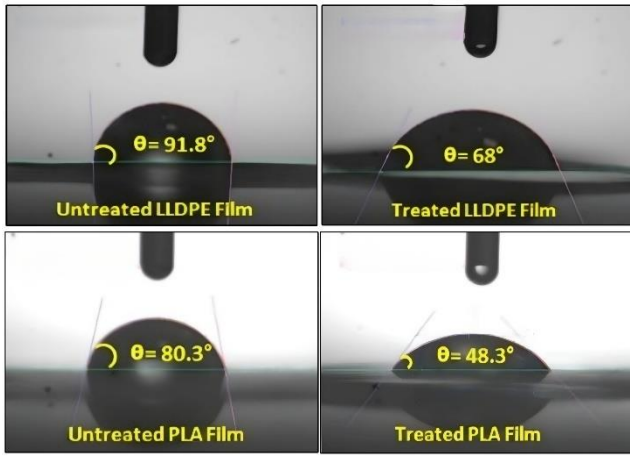


**Fig. 3.** Water CAV for untreated and treated PLA and LLDPE films

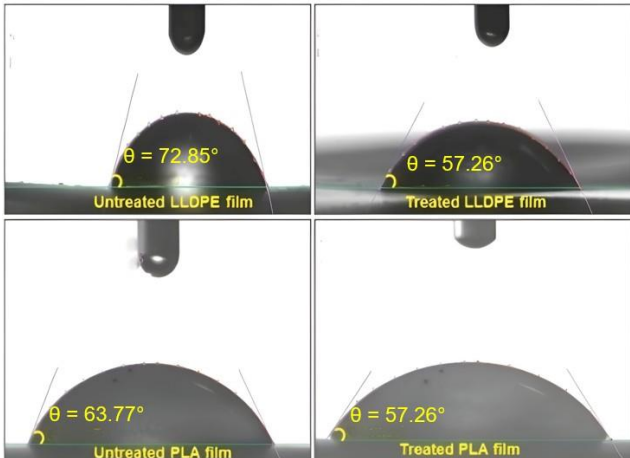


**Fig. 4.** Ethylene glycol CAV for untreated and treated PLA and LLDPE films

Ink adhesion on film substrates relies on CAV and SE. Lower CAV or higher SEL result in better ink adhesion [43]. SEL calculated by using Fowkes, Owens–Wendt and Wu models indicates that surfaces with higher CAV have lower SEL, while those with lower CAV has higher SEL. The SEL

calculated for both treated and untreated PLA and LLDPE films was shown in Table 2. In this case,  $\gamma_s^d$  and  $\gamma_s^p$  stand for the solid's polar and dispersive components of its SEL, which is the total surface energy that comprises both of these components. It has been clear that SEL calculated using Fowkes and Owens-Wendt model has the same value and closer to the practical value calculated by dyne solution testing method, but the Wu model has variation in SEL than the another two models.

**Table 2.** SEL of Treated and Untreated PLA and LLDPE

Sample	Surface energy components, mN/m								
	Fowkes Model			Wu Model			Owens-Wendt Model		
	$\gamma_s^p$	$\gamma_s^d$	$\gamma_s$	$\gamma_s^p$	$\gamma_s^d$	$\gamma_s$	$\gamma_s^p$	$\gamma_s^d$	$\gamma_s$
Untreated PLA	5.1	34.9	40	8.4	27.2	35.6	5.1	34.9	40
Treated PLA	7.0	41.0	48.0	11.2	31.2	42.4	6.7	41.3	48
Untreated LLDPE	0.25	35.77	36.0	4.80	29.50	33.5	0.25	35.77	36.0
Treated LLDPE	1.0	43.0	44.0	9.24	29.8	39.04	1.0	43.0	44.0

#### 4.1.3. Developed Fuzzy logic model for prediction of SEL for treated and untreated films

Mamdani based fuzzy inference used to predict the SEL of PLA and LLDPE treated and untreated flexible films. The linguistic factors are utilized for the fuzzy inference sets to describe the polar and dispersive components of  $SE$  [44]. The fuzzy model was developed, and the triangular membership function ( $mf$ ) has been selected for both input parameters and output parameter of untreated and treated flexible films were represented in Fig. 5 and Fig. 6. The polar components of  $SE$  are described between 0.25 to 1.8 and denoted as  $p_i = \{p_1, p_2, p_3\}$  represented in the vector form. These values are similar for both  $p_{ut}$  and  $p_t$  ( $p_{ut}$  – untreated polar component,  $p_t$  – treated polar component).

The  $mf$  equation of  $p$  is:

$$p_1(x) = \frac{1.025-x}{0.775}, \quad x \in (0.25, 1.025); \quad (7)$$

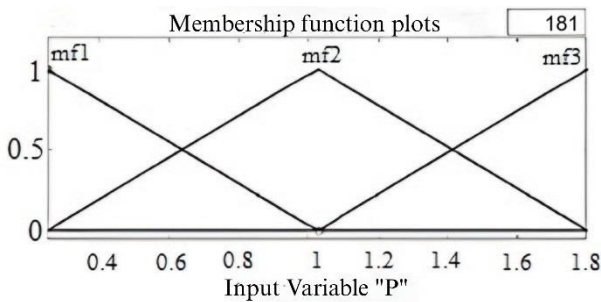
$$p_2(x) = \begin{cases} \frac{x-1.025}{0.775}, & x \in (0.25, 1.025) \\ \frac{1.8-x}{0.775}, & x \in (1.025, 1.8) \end{cases}; \quad (8)$$

$$p_3(x) = x - \frac{1.8}{0.775}, \quad x \in (1.025, 1.8). \quad (9)$$

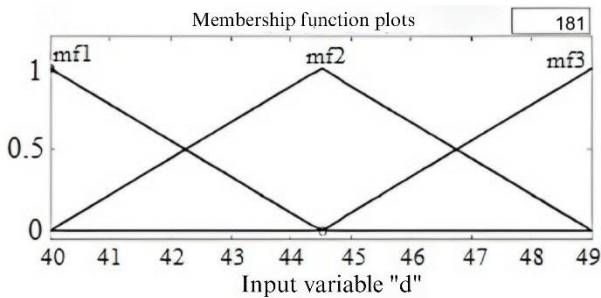
Fig. 5 a shows the  $mf$  of  $p_{ut}$  for untreated PLA and untreated LLDPE and value is 0.25 to 1.8 divided into three fuzzy sets and also denoted as  $p_{uti} = (p_{ut1}, p_{ut2}, p_{ut3})$ . Fig. 5 b shows the  $mf$  of  $d_{ut}$  for PLA and value is 40 to 49 divided into three fuzzy sets and also denoted as  $d_{uti} = (d_{ut1}, d_{ut2}, d_{ut3})$ , represented in the vector form as similar as  $p_i$ . Fig. 5 c shows the  $mf$  of  $d_{ut}$  for LLDPE and value is 34 to 40 divided into three fuzzy sets and also denoted as  $d_{utij} = (d_{ut1}, d_{ut2}, d_{ut3})$ . The output factor  $SE_{uti}$  ranges from 34 to 46 for untreated PLA and  $SE_{utij}$  ranges from 32 to 42 for untreated LLDPE divided into eight fuzzy sets and denoted as  $SE_{uti} = (SE_{ut1}, SE_{ut2}, \dots, SE_{ut8})$  and  $SE_{utij} = (SE_{ut1}, SE_{ut2}, \dots, SE_{ut8})$  represented in the vector form as similar as  $p_i$ . Fig. 5 d and e) illustrate the  $mf$  of  $SE_{uti}$  and  $SE_{utij}$  respectively. Fig. 6 a shows the  $mf$  of  $p_t$  for treated

PLA and treated LLDPE and value is 0.25 to 1.8 divided into three fuzzy sets and also denoted as  $p_{ii} = (p_{i1}, p_{i2}, p_{i3})$ . Fig. 6 b shows the mf of  $d_i$  for treated PLA and value is 40 to 49 divided into three fuzzy sets and also denoted as  $d_{ii} = (d_{i1}, d_{i2}, d_{i3})$ , represented in the vector form as similar as  $p_i$  Fig. 6 c shows the mf of  $d_i$  for treated LLPDE and value is 40 to 46 divided into three fuzzy sets and also denoted as  $d_{ij} = (d_{i1}, d_{i2}, d_{i3})$ . The output factor  $SE_{ii}$  ranges from 40 to 52 for treated PLA and  $SE_{ij}$  ranges from 40 to 48 for treated LLPDE divided into eight fuzzy sets and denoted as  $SE_{ii} = (SE_{i1}, SE_{i2}, \dots, SE_{i8})$  and  $SE_{ij} = (SE_{i1}, SE_{i2}, \dots, SE_{i8})$  represented in the vector form as similar as  $p_i$  Fig. 6 d and e) illustrate the mf of  $SE_{ii}$  and  $SE_{ij}$  respectively.

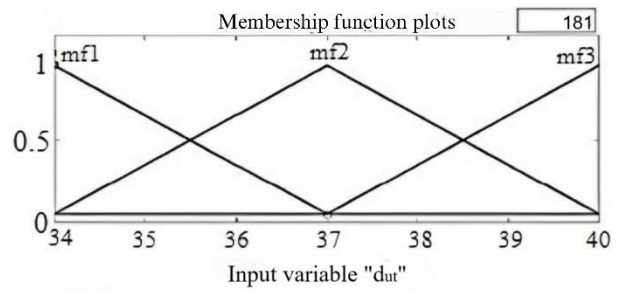
Fuzzy logic controller provides the precised output response and these set is named as defuzzification. The centre of gravity method is utilized in the defuzzification. Fig. 7 and Fig. 8 illustrate that the optimized output response of  $SE$  of flexible film along with the input parameters. The x-coordinate of the centroid was signified by using a red colour in the defuzzified value. The specific tool box in MATLAB (2021a), fuzzy logic designer was utilized for the analysis to predict the output response of  $SE$  of bio thin film. The optimized value for untreated PLA and LLPDE is observed as  $SE_{ut1} = 1.02$ ,  $SE_{ut2} = 39$ , and  $SE_{ut3} = 1.02$ ,  $SE_{ut4} = 37$  respectively (ut1 and ut3 are polar, ut2 and ut4 are dispersive). The optimal maximum  $SE_{ut}$  for untreated PLA and LLPDE is 40 and 38 respectively. From the fuzzy rule, the optimized value is observed for treated PLA as  $SE_{t1} = 1.02$  and  $SE_{t2} = 44.5$ , and the optimal maximum  $SE_{ut}$  from the fuzzy logic  $SE_t = 45.4$ . Simultaneously, the optimized value is observed for treated LLPDE as  $SE_{t3} = 1.02$ ,  $SE_{t4} = 43$  and the optimum  $SE_t = 44$  (t1 and t3 are polar, t2 and t4 are dispersive).  $R^2$  value of fuzzy logic for  $SE_{ut}$  is 0.9991 and  $SE_t$  is 0.9993. The high value of  $R^2$  (99.9 %) shows the good fitness between predicted and actual results of  $SE$  of flexible film.



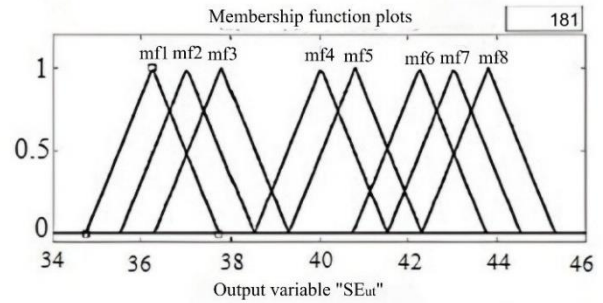
a



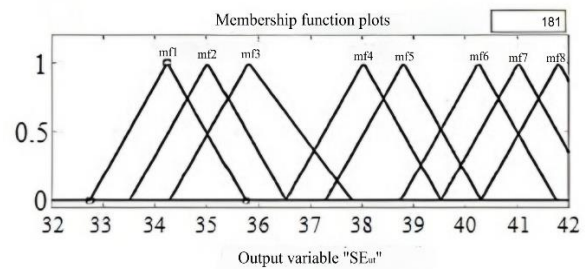
b



c

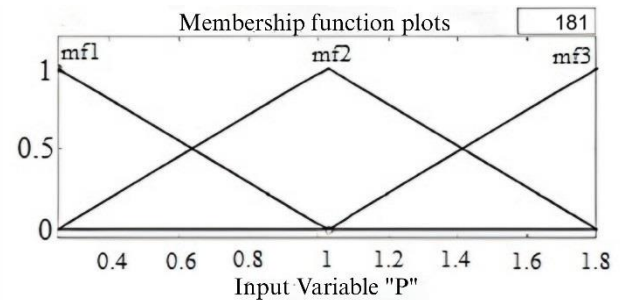


d

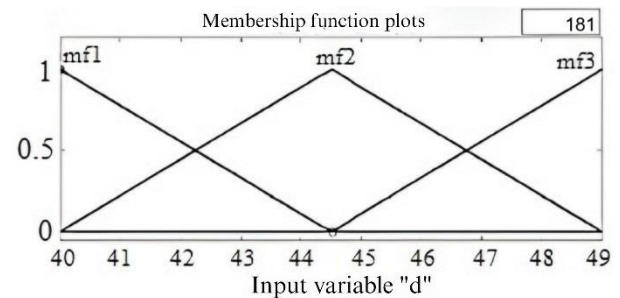


e

Fig. 5. Membership functions of polar ( $p$ ), dispersive ( $d$ ) and surface energy ( $SE$ ) for untreated PLA and LLPDE



a



b

continued on next page

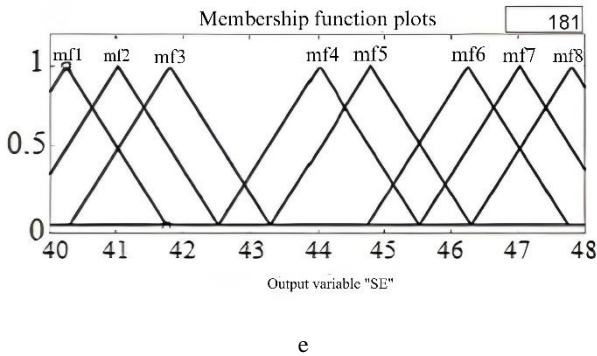
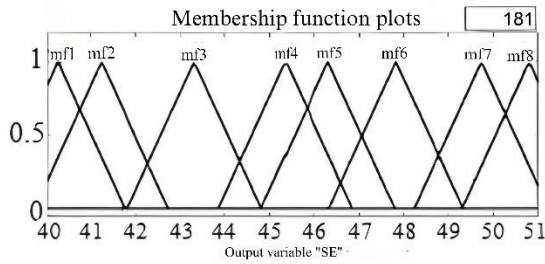
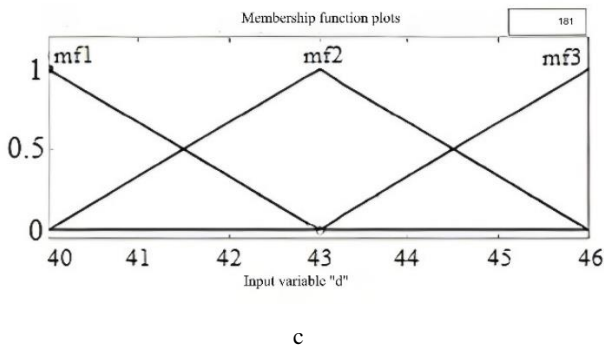


**Fig. 6.** Membership functions of polar (*p*), dispersive (*d*) and surface energy (*SE*) for treated PLA and LLDPE

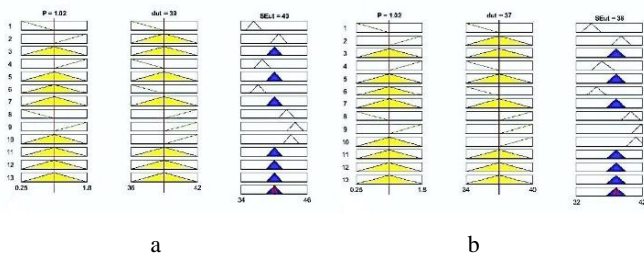


**Fig. 7.** The optimal output responses of *SE*: a–PLA-untreated; b–LLDPE-untreated

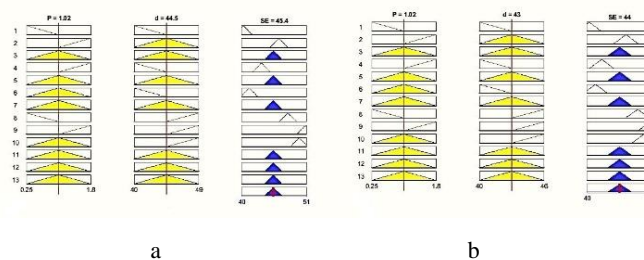


**Fig. 8.** The optimal output responses of *SE*: a–PLA-treated; b–LLDPE-treated

## 4.2. Printability analysis of flexible films

### 4.2.1. Density

In the printing industry frequently uses quinacridone (QA) as a magenta pigment. It is necessary to keep the standard density of Magenta ink for film at  $1.50 \text{ g/cm}^3$  [44]. The maximum density was found in untreated PLA film, however all printed densities exceeded this threshold. PLA film typically have higher densities than other films. Table 3 displays the density values for both treated and untreated PLA and LLDPE film. It was observed from the table data that the standard density was reached by both the treated and untreated films.

**Table 3.** Density of the films

Films	Untreated PLA	Treated PLA	Untreated LLDPE	Treated LLDPE
Average density, $\text{g/cm}^3$	1.78	1.68	1.83	1.75

### 4.2.2. Rub resistance

Both treated and untreated films' rubbing resistance was assessed using the Sutherland Ink Rub Tester (Micro Digital). The  $2 \times 4$  inch film samples were taped onto the test block after being cut into strips. Two pounds of weight were added, and the two film samples were rubbed against one another at a rate of 72 cycles per minute (CPM) as per ASTM D5264 standard. It was determined from the visual test results of the tested film samples that treated PLA and LLDPE films have greater rubbing resistance than their untreated counterparts. It was further noted that, the treated films had sufficient SEL on the film surface to retain the ink particles, as compared to the other untreated films that display ink peel off due to inadequate SEL on the film surface, as illustrated in Fig. 9.

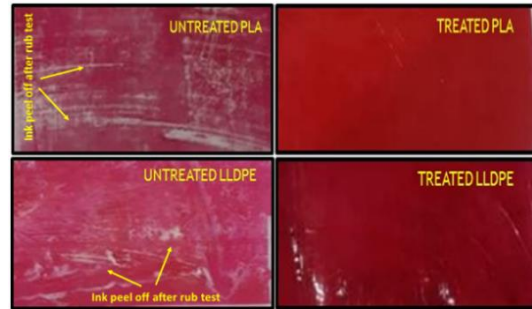


**Fig. 9.** Digital photographic image of untreated and treated PLA and LLDPE printed films before and after rub resistance test

### 4.2.3. Tape peel off adhesion test

The adhesion test was conducted using Scotch 3M premium grade transparent cellophane 610 Tape in compliance with ASTM D3359. On both treated and untreated PLA and LLDPE film, a bit two-inch strip of cellophane tape was applied, and it was quickly removed after being gently patted down.

After the experimentation, a visual test was performed on the film samples. It was observed that the treated PLA and LLDPE films showed good ink adhesion compared to non-treated PLA and LLDPE films. It was further noted that

the untreated films lacked adequate SEL to retain the ink particles and it shows ink peel off after performing the tape test, as shown in Fig. 10.

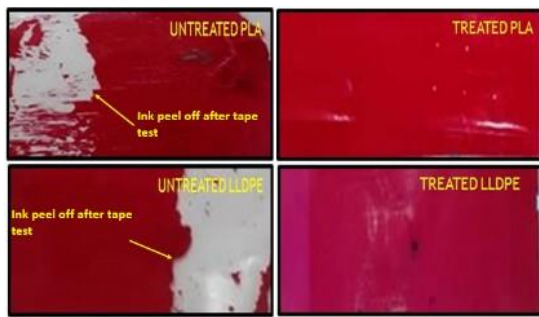


**Fig. 10.** Digital photographic image of untreated and treated PLA and LLDPE printed films before and after tape peel off test

## 5. CONCLUSIONS

The research work demonstrates that surface treatment greatly improves the SEL and printability of PLA and LLDPE films, with treated films showing notable gains in wettability and ink adhesion. The simulated SEL values closely matched the experimental ones, demonstrating the validity of the Mamdani Fuzzy Logic inference system as a predictive tool. The FL model's steady performance points to its potential for packaging applications where printing settings need to be optimized. Notably, PLA films show great promise as sustainable substitutes for traditional synthetic polymers due to their enhanced surface qualities and environmental benefits. Future packaging procedures that incorporate fuzzy logic may make the use of biopolymers in flexible packaging applications more effective and environmentally friendly.

## REFERENCES

- Luijsterburg, B., Goossens, H.** Assessment of Plastic Packaging Waste: Material Origin, Methods, Properties *Resources Conservation and Recycling* 2014: pp. 88–97. <https://doi.org/10.1016/j.resconrec.2013.10.010>
- Jacobson, J., Keif, M., Rong, X., Singh, J., Vorst, K.** Flexography Printing Performance of PLA Film *Journal of Applied Packaging Research* 3 (2) 2009: pp. 91. <https://doi.org/1557-7244/09/02091-14>.
- Rong, X., Keif, M.** A Study of PLA Printability with Flexography *In 59th Annual Technical Association of Graphic Arts Technical Conference Proceedings: Pittsburgh, PA* 2007: pp. 605–613.
- Izdebska-Podsiadly, J.** Application of Plasma in Printed Surfaces and Print Quality *In Non-Thermal Plasma Technology for Polymeric Materials* 2019: pp. 159–191. <https://doi.org/10.1016/B978-0-12-813152-7.00006-8>
- Yu, W., Hou, W.** Correlations of Surface Free Energy and Solubility Parameters for Solid Substances *Journal of Colloid and Interface Science* 544 2019: pp. 8–13. <https://doi.org/10.1016/j.jcis.2019.02.074>
- Luu, W.T., Douglas, W.B., Kettle, J., Aspler, J.** Influence of Ink Chemistry and Surface Energy on Flexographic Print Quality *In TAPPI 11th Advanced Coating Fundamentals Symposium: The Latest Advances in Coating Research and Development. Munich, Germany* 2010: pp. 309–332.
- Kim, J.Y., Heyden, S., Gerber, D., Bain, N., Dufresne, E.R., Style, R.W.** Measuring Surface Tensions of Soft Solids with Huge Contact-Angle Hysteresis *Physical Review X* 11 (3) 2021: pp.031004. <https://doi.org/10.1103/PhysRevX.11.031004>
- Owens, D.K., Wendt, R.C.** Estimation of the Surface Free Energy of Polymers *Journal of Applied Polymer Science* 13 (8) 1969: pp. 1741–1747. <https://doi.org/10.1002/app.1969.070130815>
- Tuominen, M., Lahti, J., Lavonen, J., Penttinen, T., Räsänen, J.P., Kuusipalo, J.** The Influence of Flame, Corona and Atmospheric Plasma Treatments on Surface Properties and Digital Print Quality of Extrusion Coated Paper *Journal of Adhesion Science and Technology* 24 (3) 2010: pp. 471–492. <https://doi.org/10.1163/016942409X12561252292224>
- Strobel, M., Lyons, C.S., Strobel, J.M., Kapaun, R.S.** Analysis of Air-Corona-Treated Polypropylene and Poly (Ethylene Terephthalate) Films by Contact-Angle Measurements and X-Ray Photoelectron Spectroscopy *Journal of Adhesion Science and Technology* 6 (4) 1992: pp. 429–443. <https://doi.org/10.1163/156856192X00764>
- Morsy, F.A., Elsayad, S.Y., Bakry, A., Eid, M.A.** Surface Properties and Printability of Polypropylene Film Treated by an Air Dielectric Barrier Discharge Plasma *Surface Coating's International Part B* 89 (1) 2006: pp. 49. <https://doi.org/10.1007/BF02699614>
- Sarkara, S., Mandala, R., Mondal, N., Chaudhric, S., Mandal, T., Majumdar, G.** Modelling and Prediction of Micro-Hardness of Electroless Ni-P Coatings Using Response Surface Methodology and Fuzzy Logic *Jordan Journal of Mechanical and Industrial Engineering* 16 (5) 2022: pp. 729–742.
- Peršin Fratnik, Z., Plohl, O., Kokol, V., Fras Zemljič, L.** Using Different Surface Energy Models to Assess the Interactions Between Antiviral Coating Films and phi6 Model Virus *Journal of Functional Biomaterials* 14 (4) 2023: pp. 232. <https://doi.org/10.3390/jfb14040232>
- Tian, W., Zhao, F., Min, C., Feng, X., Liu, R., Mei, X., Chen, G.** Broad Learning System Based on Binary Grey Wolf Optimization for Surface Roughness Prediction in Slot Milling *IEEE Transactions on Instrumentation and Measurement* 71 2022: pp. 1–10. <https://doi.org/10.1109/TIM.2022.3144232>
- Lai, F., Tong, S.** Artificial Neural Network-Based Approach for Surface Energy Prediction *Recent Advances in Neuromorphic Computing* 7 2024: pp. 1–15. <https://doi.org/10.5772/intechopen.1006093>
- Sinha, A.K., Narang, H.K., Bhattacharya, S.** Mechanical Properties of Hybrid Polymer Composites: A Review *Journal of the Brazilian Society of Mechanical Sciences and Engineering* 42 (8) 2020: pp. 431. <https://doi.org/10.1007/s40430-020-02517-w>
- Almtori, S.A., Al-Fahad, I.O.B., Al-temimi, A.H.T., Jassim, A.K.** Characterization of Polymer based composite Using Neuro-Fuzzy Model *Materials Today: Proceedings* 42 2021: pp. 1934–1940. <https://doi.org/10.1016/j.matpr.2020.12.238>
- Masood, A., Ahmad, K.** A Review on Emerging Artificial Intelligence (AI) Techniques for Air Pollution Forecasting: Fundamentals, Application and Performance *Journal of Cleaner Production* 322 2021: pp. 129072. <https://doi.org/10.1016/j.jclepro.2021.129072>



19. **Mandala, R., Majumdara, G.** Modelling and Prediction of Micro-Hardness of Electroless Ni-P Coatings Using Response Surface Methodology and Fuzzy Logic *Jordan Journal of Mechanical and Industrial Engineering* 16 (5) 2022: pp. 729–742
20. **Rajamani, D., Esakki, B., Arunkumar, P., Velu, R.** Fuzzy Logic-Based Expert System for Prediction of Wear Rate in Selective Inhibition Sintered HDPE Parts *Materials Today: Proceedings* 5 (2) 2018: pp. 6072–6081.  
<https://doi.org/10.1016/j.matpr.2017.12.212>
21. **Nayak, S.K., Satapathy, A., Mantry, S.** Tribological Evaluation of Marble Dust Filled Polyester Composites Using an Integrated Fuzzy Logic and Response Surface Method Approach *Materials Today: Proceedings* 62 2022: pp. 6163–6170.  
<https://doi.org/10.1016/j.matpr.2022.05.039>
22. **Dey, A.S., Ashok, S.D.** Fuzzy Logic Based Qualitative Indicators for Promoting Extended Producer Responsibility and Sustainable Food Packaging Waste Management *Environmental and Sustainability Indicators* 24 2024: pp. 100534.  
<https://doi.org/10.1016/j.indic.2024.100534>
23. **Paturi, U.M.R., Rishika Reddy, M., Pranodh Reddy, G.** Estimation of Surface Roughness Using Artificial Neural Networks and Fuzzy Logic During Extrusion-Based 3D Printing *In AIP Conference Proceedings* 2754 (1) 2023: pp. 1–15  
<https://doi.org/10.1063/5.0161130>
24. **Repeta, V., Kukura, T., Havrylyshyn, V., Kukura, Y.** Analysis of Factors and Construction of Prognostic Quality Models of Flexographic Printing Process of Packaging With Solvent Based Inks *Journal of Graphic Engineering and Design* 14 (3) 2023: pp. 37–44.  
<https://doi.org/10.24867/JGED-2023-3-037>
25. **Maiti, S., Islam, M.R., Uddin, M.A., Afroj, S., Eichhorn, S.J., Karim, N.** Sustainable Fiber-Reinforced Composites: A Review *Advanced Sustainable Systems* 6 (11) 2022: pp. 2200258.  
<https://doi.org/10.1002/adsu.202200258>
26. **Venkatesan, R., Rajeswari, N., Thendral Thiyagu, T.** Preparation, Characterization, and Mechanical Properties of K-Carrageenan/ SiO<sub>2</sub> Nanocomposite Films for Antimicrobial Food Packaging *Bulletin of Materials Science* 40 2017: pp. 609–614.  
<https://doi.org/10.1007/s12034-017-1403-3>
27. **Ataefard, M.** Study of PLA Printability with Flexography Ink: Comparison with Common Packaging Polymer *Progress in Color, Colorants and Coatings* 12 (2) 2019: pp. 101–105.  
<https://doi.org/10.30509/pccc.2019.81545>
28. **Thiyagu, T.T., Gokilakrishnan, G., Uvaraja, V.C., Maridurai, T., Prakash, V.A.** Effect of SiO<sub>2</sub>/TiO<sub>2</sub>, and ZnO Nanoparticle on Cardanol Oil Compatibilized PLA/PBAT Biocomposite Packaging Film *Silicon* 14 (7) 2022: pp. 3795–3808.  
<https://doi.org/10.1007/s12633-021-01577-4>
29. **Sousa, A.F., Patrício, R., Terzopoulou, Z., Bikiaris, D.N., Stern, T., Wenger, J., Guigo, N.** Recommendations for Replacing PET on Packaging, Fiber, and Film Materials with Biobased Counterparts *Green Chemistry* 23 (22) 2021: pp. 8795–8820.  
<https://doi.org/10.1039/D1GC02082J>
30. **Hansuebsai, A., Nawakitwong, S.** Printability Analysis of Compostable Films by Flexographic Water Based Ink *Key Engineering Materials* 843 2020: pp. 26–32.  
<https://doi.org/10.4028/www.scientific.net/KEM.843.2>
31. **Chen, H., Liu, Y., Balabani, S., Hirayama, R., Huang, J.** Machine Learning in Predicting Printable Biomaterial Formulations for Direct Ink Writing *Research* 6 2023: pp. 0197.  
<https://doi.org/10.34133/research.0197>
32. **Ozdemir, B., Hernández-del-Valle, M., Gaunt, M., Schenk, C., Echevarría-Pastrana, L., Fernandez-Blazquez, J.P., Haranczyk, M.** Advancing the Prediction of 3D Printability for Polymer Nanocomposites *ChemRxiv* 2024: pp. 1–35.  
<https://doi.org/10.26434/chemrxiv-2024-33788>
33. **Espino, M.T., Tuazon, B.J., Espera, Jr.A.H., Noheseda, C.J.C., Manalang, R.S., Dizon, J.R.C., Advincula, R.C.** Statistical Methods for Design and Testing of 3D-Printed Polymers *MRS Communications* 13 (2) 2023: pp. 193–211.  
<https://doi.org/10.1557/s43579-023-00332-7>
34. **Nasrin, T., Pourali, M., Pourkamali-Anaraki, F., Peterson, A.M.** Active Learning for Prediction of Tensile Properties for Material Extrusion Additive Manufacturing *Scientific Reports* 13 (1) 2023: pp. 11460.  
<https://doi.org/10.1038/s41598-023-38527-6>
35. **Saleh, B., Maher, I., Abdelrhman, Y., Heshmat, M., Abdelaal, O.** Adaptive Neuro-Fuzzy Inference System for Modelling the Effect of Slurry Impacts on PLA Material Processed by FDM *Polymers* 13 (1) 2020: pp. 118.  
<https://doi.org/10.3390/polym13010118>
36. **Di Cerbo, A., Mescola, A., Rosace, G., Stocchi, R., Rossi, G., Alessandrini, A., Preziuso, S., Scarano, A., Rea, S., Loschi, A.R., Sabia, C.** Anti-Bacterial Effect of Stainless-Steel Surfaces Treated with a Nanotechnological Coating Approved for Food Contact *Microorganisms* 9 (2) 2021: pp. 248.  
<https://doi.org/10.3390/microorganisms9020248>
37. **Kozbial, A., Li, Z., Conaway, C., McGinley, R., Dhingra, S., Vahdat, V., Zhou, F., D’Urso, B., Liu, H., Li, L.** Study on the Surface Energy of Graphene by Contact Angle Measurements *Langmuir* 30 (28) 2014: pp. 8598–8606.  
<https://doi.org/10.1021/la5018328>
38. **Ahadian, S., Mohseni, M., Moradian, S.** Ranking Proposed Models for Attaining Surface Free Energy of Powders Using Contact Angle Measurements *International Journal of Adhesion & Adhesives* 29 2009: pp. 458–469.  
<https://doi.org/10.1016/j.ijadhadh.2008.09.004>
39. **Fowkes, F.M.** Attractive Forces at Interfaces *Industrial & Engineering Chemistry* 56 (12) 1964: pp. 40–52.  
<https://doi.org/10.1021/ie50660a008>
40. **Wu, S.** Calculation of Interfacial Tension in Polymer Systems *In Journal of Polymer Science Part C: Polymer Symposia* 34 (1) 1971: pp. 19–30.  
<https://doi.org/10.1002/polc.5070340105>
41. **Elerian, F. A.** A New Fuzzy Logic Approach for Prediction of Surface Roughness *Mej-Mansoura Engineering Journal* 45 (3) 2020: pp. 50–56.  
<https://doi.org/10.21608/BFEMU.2020.118051>
42. **Mohamed, R.A.** Modelling of Dielectric Behaviour of Polymers Nanocomposites Using Adaptive Neuro-Fuzzy Inference System (ANFIS) *The European Physical Journal Plus* 137 (3) 2022: pp. 384.  
<https://doi.org/10.1140/epjp/s13360-022-02518-9>
43. **Das, B., Chakrabarty, D., Guha, C., Bose, S.** Effects of Corona Treatment on Surface Properties of Coextruded

Transparent Polyethylene Film *Polymer Engineering & Science* 61 (5) 2021: pp. 1449–1462.  
<https://doi.org/10.1002/pen.25663>

Formulated for Maximum Color Gamut *Color Research & Application* 45 (6) 2020:pp. 1153–1169.  
<https://doi.org/10.1002/col.22552>

44. **Borenstain, S., Bar Haim, G., Goldshtein, K., Cohen Taguri, G.** Optimization of Quinacridone Magenta, Cu-Phthalocyanine Cyan, and Arylide Yellow Ink Films



© Elangovan et al. 2025 Open Access This article is distributed under the terms of the Creative Commons Attribution 4.0 International License (<http://creativecommons.org/licenses/by/4.0/>), which permits unrestricted use, distribution, and reproduction in any medium, provided you give appropriate credit to the original author(s) and the source, provide a link to the Creative Commons license, and indicate if changes were made